ORIGINAL ARTICLE

Mechanically Reinforced Extracellular Matrix Scaffold for Application of Cartilage Tissue Engineering

Hyun Ju Oh[1] · Soon Hee Kim[2] · Jae-Ho Cho[3] · Sang-Hyug Park[4] · Byoung-Hyun Min[1,2,3,5]

Abstract Scaffolds with cartilage-like environment and suitable physical properties are critical for tissue-engineered cartilage repair. In this study, decellularized porcine cartilage-derived extracellular matrix (ECM) was utilized to fabricate ECM scaffolds. Mechanically reinforced ECM scaffolds were developed by combining salt-leaching and crosslinking for cartilage repair. The developed scaffolds were investigated with respect to their physicochemical properties and their cartilage tissue formation ability. The mechanically reinforced ECM scaffold showed similar mechanical strength to that of synthetic PLGA scaffold and expressed higher levels of cartilage-specific markers compared to those expressed by the ECM scaffold prepared by simple freeze-drying. These results demonstrated that the physical properties of ECM-derived scaffolds could be influenced by fabrication method, which provides suitable environments for the growth of chondrocytes. By extension, this study suggests a promising approach of natural biomaterials in cartilage tissue engineering.

Keywords Extracellular matrix scaffold · Scaffold fabrication · Cartilage regeneration · Chemical crosslinking

✉ Sang-Hyug Park
shpark1@pknu.ac.kr

✉ Byoung-Hyun Min
dr.bhmin@gmail.com

1   Department of Molecular Science and Technology, Ajou University, 206, World Cup-ro, Yeongtonggu, Suwon 16499, Korea

2   Cell Therapy Center, Ajou University Medical Center, Ajou University, 206, World Cup-ro, Yeongtonggu, Suwon 16499, Korea

3   Department of Orthopedic Surgery, School of Medicine, Ajou University, 206, World Cup-ro, Yeongtonggu, Suwon 16499, Korea

4   Department of Biomedical Engineering, Pukyong National University, 45, Yongso-ro, Namgu, Busan 48513, Korea

5   Department of Orthopedic Surgery, School of Medicine, Ajou University, 206, World Cup-ro, Yeongtonggu, Suwon 16499, Korea

1 Introduction

Hyaline cartilage extracellular matrix (ECM) is consisting of a complex structural network of collagen and proteoglycans and show the antiangiogenic effects [1]. The limited blood supply in cartilage is thought to be responsible for its limited capacity for self-repair; thus, cartilage defect cannot be naturally regenerated. In particular, damaged cartilage may cause pain and disability; therefore, Numerous techniques have been developed to repair articular cartilage damage, a typical example being tissue engineering, a promising way to restore functional hyaline cartilage in joints [2, 3].

The essential approach to tissue engineering requires the use of cells, three-dimensional (3D) porous scaffolds, and stimulating factors, which can be used alone or in combination with others [4, 5].

Engineered scaffolds are vitally important for articular cartilage regeneration. An ideal scaffold for cartilage repair should demonstrate the native cartilage comparable mechanical properties, promote the synthesizing of

cartilage ECM, and prove the integration with the surrounding host tissue [6]. Materials composing scaffolds and inner structures could play a major role in dictating cellular behavior and ultimately affect cartilage tissue formation and functionality [7–9]. Therefore, to date, a wide range of natural and synthetic materials such as hydrogels, sponges, and fibrous meshes have been investigated as scaffolds for cartilage repair [10–13]. In particular, tissue-derived ECM materials harvested from various sources of tissues, such as skin, small intestinal submucosa, urinary bladder, blood vessels, and heart valves, have been used as scaffolds for the repair of many tissues [14–16]. Cartilage-derived ECM of cows, pigs, and humans have been developed and used for cartilage regeneration [17, 18]. We have also already compared collagen and cartilage ECM materials and found the latter to be more favorable for cartilage regeneration [19].

Scaffolds fabricated for cartilage tissue engineering usually possess a porous structure. Porous 3D scaffolds aid the attachment, growth, and differentiation of cells inside the material and are expected to degrade gradually and be replaced with regenerated and completely functional tissue [20–22]. Several methods including porogen leaching, freeze-drying, and gas-foaming can be employed to manufacture 3D porous sponges, and these manufacturing methods affect scaffold architecture, which influences tissue formation [3, 23]. Many research studies commonly employ a freeze-drying method for the fabrication of ECM scaffolds. However, freeze-dried ECM sponge scaffolds showed delicate mechanical properties [7, 24, 25].

Our hypothesis is that the physical properties of ECM scaffolds could be improved by modifying the fabrication process. Mechanically improved ECM scaffolds would ultimately upregulate chondrogenic tissue formation. In this study, we fabricated mechanically reinforced ECM scaffolds using a process that combines solvent-casting/salt-leaching and chemical double crosslinking. The physical and chemical properties of the mechanically reinforced ECM scaffolds were evaluated, and *in vitro* chondrogenesis on these scaffolds was compared to that on both, poly (lactic-co-glycolic acid) (PLGA) prepared by solvent-casting/salt-leaching and ECM scaffolds prepared by simple freeze-drying.

2 Materials and methods

### 2.1 Preparation of porcine cartilage-derived ECM powder (PCP)

Full-thickness porcine cartilage was harvest from femoral condyles of 6-month-old porcine knee joints immediately within 1 h after sacrifice. Cartilage was finely minced using

scalpels (2 cm × 3 cm) and washed with phosphate-buffered saline (PBS, Gibco BRL, Grand Island, NY, USA) at pH 7.4 three times for 10 min. The washed cartilage pieces were frozen in PBS complemented with 1% antibiotics (100 U/mL penicillin and 100 mg/mL streptomycin, Sigma) at − 80 °C. Fragments were ground using a commercial mixer (Hood Mixer HMF-505, Hanil, Korea) to a size of 2 mm × 2 mm. These grains were then lyophilized and pulverized using a cryogenic laboratory mill (JAI, JFC-300, Japan) in liquid nitrogen. Cartilage powder was decellularized under aseptic conditions as follows. 10 g of powder was stirred in 1 L of 0.1% sodium dodecyl sulfate (SDS, Bio-Rad, USA) at 100 rpm for 24 h. After SDS treatment, the suspension of cartilage powders was centrifuged for 1 h at 10,000 rpm. The deposit was treated with 200 mL of 200 U/mL DNase (Sigma, USA) for 24 h with stirring at 100 rpm at 37 °C. After treatment, it was washed with distilled water five times for 30 min each. The exchange of washing solution was carried out in the same way as SDS removal. Prepared decellularized porcine cartilage-derived matrix powder (PCP) was lyophilized and stored at − 20 °C until use. DNA contents in the biomaterial were analyzed using DNA quantitative equipment (Qubic, Bio-Rad, USA).

2.2 Preparation of PLGA, PCP-br, and PCP-sp scaffolds

We denoted the mechanically reinforced PCP scaffold as "brick-type PCP scaffold" (PCP-br). The complete fabrication process is illustrated in Fig. 1. To fabricate PCP-br, 9 g of sodium chloride (NaCl) particles in the range of 250–350 μm was were with 1 g of PCP. Next, 2 mL of 1 M *N*-(3-dimethylaminopropyl)-*N*-ethylcarbodiimide hydrochloride (EDC, Sigma, USA) in ethanol was added into the mixture of NaCl and PCP to solidify and precrosslink. This EDC solution was poured into a circular disk-like cemented carbide mold (diameter: 5 mm, thickness: 2 mm) and the mold was pressurized to 1000 psi at room temperature for 10 s (Shinpyung, Press Hydraulic, Korea). To fabricate the "sponge-type PCP scaffold" (PCP-sp), the obtained PCP (1% concentration) was added to a vial with 10 mL of distilled water adjusted to pH 3 using HCl, followed by stirring for 24 h. This PCP sol was neutralized by NaOH and carefully poured into a homemade silicone molder (diameter: 5 mm, thickness: 2 mm). Then, the PCP sol was frozen at − 20 °C and freeze-dried to become PCP-sp. PCP-br and PCP-sp were crosslinked with 100 mM EDC in deionized water and ethanol (5/95 v/v) and 100 mM *N*-hydroxysuccinimide (NHS, Fluka, Japan) for 4 h. After crosslinking, the resulting scaffolds were washed with 0.1 M Na_2HPO_4 solution to cease the cross-linking reaction and were immersed in deionized
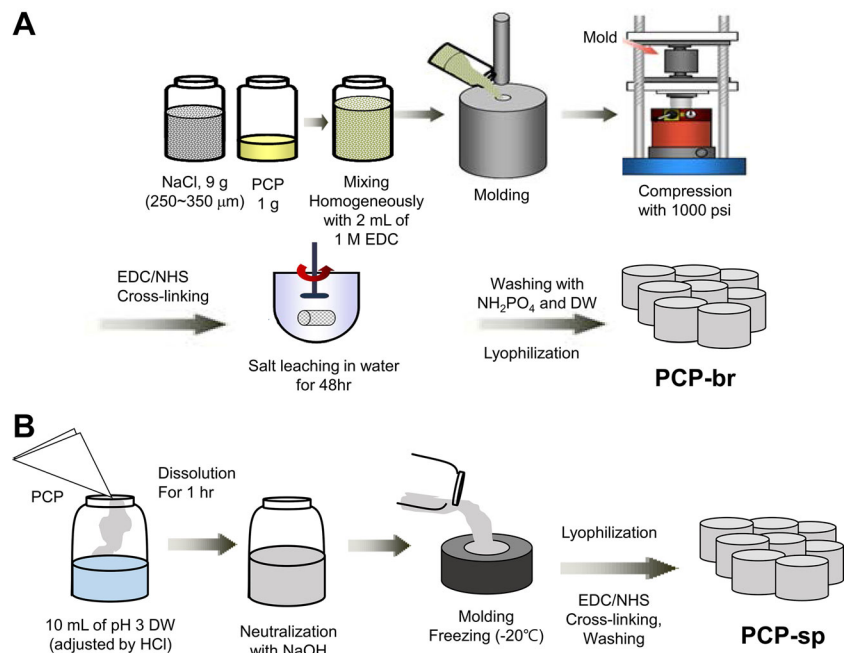
water, which was changed every 6 h over a 48-h period to leach out NaCl (for PCP-br) and remove the crosslinker. The PCP scaffolds were washed three times with NH_2PO_4 and distilled water, followed by freeze-drying.

Porous PLGA scaffolds were prepared by a solvent-casting/salt-leaching method. PLGA (molecular weight: 90,000 g/mol, lactide to glycolide mole ratio of 75:25, Resomer® RG 756) was purchased from Boehringer Ingelheim (Ingelheim, Germany). 1 g of PLGA was dissolved in 10 mL of methylene chloride (Samchun Chemical, Korea), and 9 g of NaCl particles (250–350 μm) were added. This solution was molded, pressured, and salt-leached in the same condition as those for PCP-br. The scaffolds were then freeze-dried. All scaffolds were sterilized with 70% ethanol at room temperature for 1 h before cell seeding.

2.3 Fourier-transform infrared spectroscopy (FTIR) analysis

FTIR (Bio-Rad Digilab FTS165, Canada) analysis was carried out to evaluate intermolecular cross-linkage in the PCP scaffolds before and after crosslinking with EDC/NHS. Distribution patterns of cartilage collagen related peaks were analyzed [26, 27]. The KBr pellet method was used in the analysis.

2.4 Pore characterization

A mercury intrusion porosimeter (Model AutoPore II 9220, Micromeritics Co. Ltd., USA) was utilized to analyze pore

size distributions and median pore diameter. Solid penetrometer volume was fixed to 3.6 mL and 0.0193 g of sample was examined. Mercury was filled at a filling pressure of 0.17 psi and intruded to a maximum intrusion volume of 100 mL/g. The evacuation pressure was 50 μm/Hg and evacuation time was 5 min. The porosimeter was supplied with a computer-based acquisition system that generated data files on cumulative and incremental volumes of intruded mercury as a function of pore size.

2.5 Scanning electron microscope (SEM)

SEM (JEOL, JSM-6380, Japan, 20 kV) was utilized to observe the surface of PCP and the cross-sectional morphology of the scaffolds. Sharp razor sliced samples were mounted on metal stubs with double-sided tape and coated with platinum for 30 s under argon atmosphere using a plasma sputter (SC 500 K, Emscope, UK). In the case of cell-seeded scaffolds, fixing steps were performed before cutting the samples. The cell-seeded scaffold complexes were washed with PBS and fixed with 2.5% glutaraldehyde (Sigma, USA) in PBS for 24 h at room temperature. After thorough washing with PBS, the cells on the surfaces were dehydrated in a graded series of ethanol (from 50 to 100%) for 10 min each and allowed to dry on a clean bench at room temperature.

2.6 Wetting properties

The wettability of the scaffold surface and the contact angle on the scaffold surface were evaluated. For

wettability, briefly, 100 μL of 0.01% (w/v) trypan blue aqueous solution was carefully dropped on the prepared scaffolds and photographed to record the degree of permeation in 0, 90, and 120 min. The water contact angles of the scaffolds were measured using a contact angle goniometer (SEO-300A; SEO Co., Korea). The measurement was completed within 30 s for all scaffolds. The angle between the baseline and the droplet was directly visualized on-screen using the goniometer.

2.7 Mechanical testing

Material characterization instrument (Food Technology Corporation, Texture Lab Pro, Sterling, VA, USA) was used for the evaluation of the compression strength of the scaffold only and cell-seeded scaffold. The compression strength test was conducted with a target distance to specimen of 3 mm, test speed 0.4 mm/s, and trigger force of 0.02 N with a strain of 20%.

2.8 Isolation and culture of young chondrocytes from humans in scaffolds

Young chondrocytes from humans were obtained from polydacty digits of male and female babies aged $\sim$ 3 years. All experimental protocols were approved by the Institutional Review Board at Ajou University (Approval No. AJIRB-MED-SMP-10-266). Cartilage tissues were chopped into small pieces and fused upon 16 h of incubation at 37 °C in 0.1% type II collagenase (10 mL of solution per gram of tissue, 300 U/mg, Worthington Biochemical Corporation, Lakewood, NJ, USA) and resuspended in Dulbecco's modified Eagle's medium (DMEM, Hyclone). Using a cell strainer (100 μm Nylon; Falcon), the cells were filtered and centrifuged at 1700 rpm for 10 min. Isolated cells were cultured on culture dishes in DMEM supplemented with 10% (v/v) fetal bovine serum, 50 μg/mL streptomycin, and 50 units/mL penicillin at 37 °C in an incubator with 5% CO_2.

For cell seeding in scaffolds, the scaffolds were placed individually into the wells of a 24-well tissue culture plate and washed with culture medium. After medium suction, chondrocytes at passage 2 were statically seeded into the scaffolds at a cell density of 5×10^6 cells/scaffold. Cell-scaffold complexes were transferred to a new well plate to exclude cells that were not attached to the scaffolds after 4 h. Cell-scaffold complexes were cultured with DMEM supplement with 1% antibiotic–antimycotic, 1.0 mg/mL insulin, 0.55 mg/mL human transferrin, 0.5 mg/mL sodium selenite, 50 μg/mL ascorbic acid, 1.25 μg/mL bovine serum albumin, 100 nM dexamethasone, and 40 μg/mL proline.

2.9 Measurement of glycosaminoglycan (GAG) levels

Total GAG content was determined quantitatively using the 1,9-dimethylmethylene blue (DMMB) assay. Tissues or scaffolds were frozen in a freezer and lyophilized. The lyophilized samples were homogenized thoroughly in a papain solution using a homogenizer. Fifty microliters of individual samples were mixed with 200 μL of DMMB solution (mixed buffer of Na_2HPO_4, 5 mM EDTA, 40 mM NaCl, 40 mM glycine, and 46 μM DMMB at pH 3) and the absorbance was measured at a wavelength of 525 nm by UV–visible spectroscopy (Tecan, Infinite M200). The total GAG content of each sample was extrapolated using a standard plot of shark chondroitin sulfate (Sigma, St Louis, MO, USA) with concentrations in the range of 0–50 μg/mL.

2.10 Reverse-transcriptase polymerase chain reaction (RT-PCR) analysis

Total cellular RNA was extracted using an RNA easy-spin kit (Intron, 17221, Korea) following the manufacturer's instructions. A total of 1 μg of RNA was used for cDNA synthesis using First-strand cDNA Synthesis Kit for RT-PCR (AMV) (Rhoche, 1-483-188, Germany) and 1 μg of the synthesized cDNA was used for polymerase chain reaction (PCR). PCR was performed under linear conditions using the following cycle profile: initial incubation (5 min at 94 °C); followed by 30 cycles of annealing (1 min at 50 °C to 60 °C), extension (1 min at 72 °C), and denaturation (1 min at 94 °C); and termination (5 min at 72 °C). PCR products were separated on a 1.5% agarose gel and stained with ethidium bromide. Then they were visualized and digitalized with Image Analysis System, Gel (Geliance 200, PerkinElmer®, UK). Oligonucleotide primers were used for the following human housekeeping genes: glyceraldehyde-6-phosphate dehydrogenase (GAPDH), rabbit type II collagen, and aggrecan core protein. The gene expressions of aggrecan and type II collagen were determined relative to that obtained for GAPDH.

2.11 Morphological analysis and volume measurement

After completion of the *in vitro* experiment, the macrograph of neocartilage tissue was obtained, which included morphology, color, and firmness by the gross and pinch tests.

2.12 Histology

The retrieved constructs were fixed in 4% formaldehyde for 48 h, dehydrated, and then embedded in paraffin wax. Sections of 4 μm in thickness were stained with Safranin O to identify GAGs in the matrix.

2.13 Statistical analysis

The paired t test was used to determine statistical significance, with $p < 0.05$ considered as significant.

3 Results

3.1 Characterization of PCP

Decellularization of PCP materials was carried out to eliminate the xenogeneic cellular antigens. Figure 2 shows the images of porcine knee cartilage (Fig. 2A) and the gross/surface morphology of decellularized PCP powder (Fig. 2B). PCP has a round shape and rough surface, and its diameter was analyzed to be around 50 μm by SEM (Fig. 2C). Figure 2D shows that decellularized PCP contained very low DNA content (9.48 ng/mg) compared to native cartilage (485 ng/mg), while decellularized cartilage tissue contained a relatively high DNA content of 394 ng/mg.

3.2 Physical and chemical properties of scaffolds

Figure 3 shows the chemical and physical properties of PCP-br. The FTIR spectra obtained from pure PCP and EDC/NHS-crosslinked PCP-br are shown in Fig. 3A. Pure PCP shows spectra similar to those of common cartilage collagen including a band at the frequency of 985–1140 cm^{-1} that usually appears in carbohydrate region. The frequencies of functional bands of type II collagen in PCP-br were compared to those of pure PCP. In the results, the amide A band at the 3290 cm^{-1}, which indicates NH stretch coupled with hydrogen bond was slightly shifted to 3282 cm^{-1}. However, the amide B band (2937 cm^{-1}) for representing CH$_2$ asymmetrical stretch, the amide I band (1629 cm^{-1}) for indicating C=O stretch/hydrogen bond coupled with COO$^-$ were not shifted after crosslinking. Moreover, the amide II and III bands for
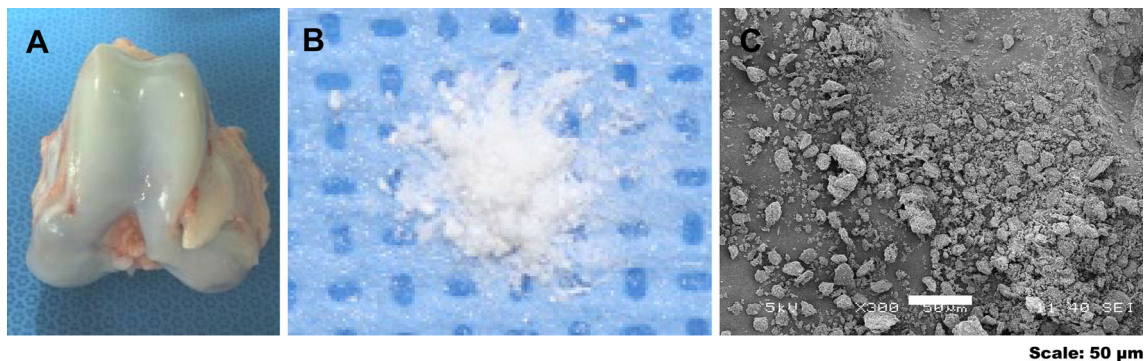

Fig. 2 Preparation of porcine cartilage-derived extracellular matrix powder (PCP). A Knee cartilage harvested from 6-month-old porcine knee joints. B Gross appearance of physicochemically treated PCP. C SEM images of decellularized PCP (scale bar: 50 μm). D Total DNA contents after decellularization based on specimen status (***$p < 0.001$)
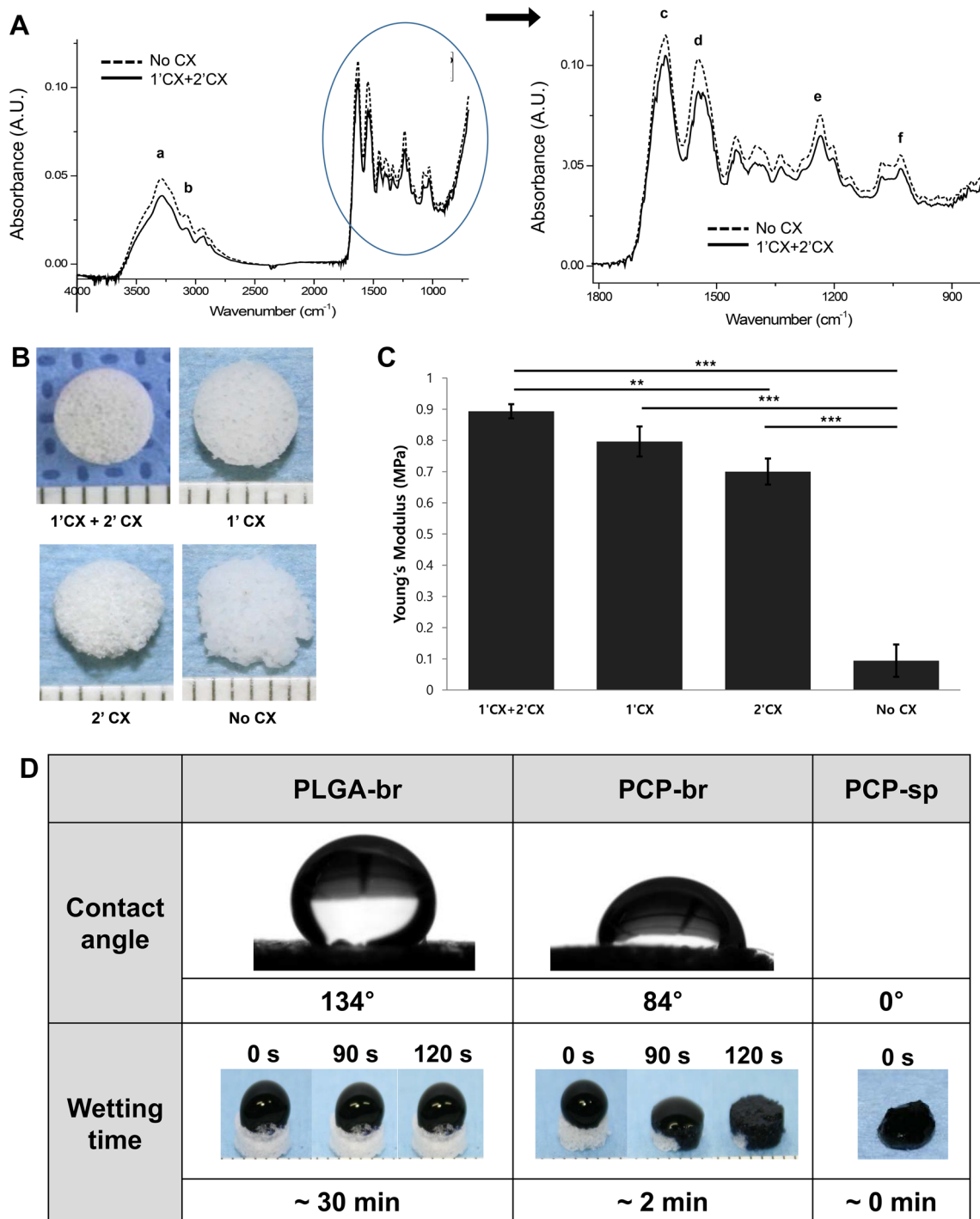
Fig. 3 Scaffold characterization. **A** Comparison of the FTIR spectra of pure PCP and crosslinked PCP-br (*a* amide A, *b* amide B, *c* amide I, *d* amide II, *e* amide III, *f* carbohydrate region). **B** Gross observation of PCP-br by CX process (1′CX: pre-crosslinking, 2′CX: post-crosslinking). **C** Mechanical strength of PCP-br by CX process. **D** Wettability of PLGA-br, PCP-br, and PCP-sp

indicating NH bend coupled with CN stretch were 1546 and 1236 cm^{-1} without no shifting. Some of minor peaks for CH$_2$ side chain of collagen and asymmetric bending of CH$_3$ also showed no changes with 1336 and 1448 cm^{-1}, respectively. Therefore, distribution patterns of cartilage

collagen related peaks were similar before and after crosslinking.

The crosslinking times affected the mechanical strength and integrity of the scaffolds. When double crosslinking was performed, the scaffold integrity improved compared to that of single-crosslinked scaffold or non-crosslinked

scaffold as shown in Fig. 3B. The compressive strength of PCP-br was 0.08 MPa before crosslinking and 0.89 MPa after crosslinking as shown in Fig. 3C. The compressive strength of crosslinked PCP-br was superior to those of the PLGA-br (0.44 MPa) and PCP-sp (0.01 MPa). This value was similar to it of native articular cartilage (0.78 Mpa) in basic study. (Supplementary figure 1).

The water contact angle on scaffolds was measured in order to compare the wetting properties among the scaffolds, and the obtained values were 134° for PLGA and 84° for PCP-br, immediately after water dropping (Fig. 3D). With the purpose of further comparing the hydrophilic properties of the PCP scaffolds, a trypan blue solution was dropped on the surfaces of the scaffolds and photographs were taken over time. PCP-based scaffolds soaked up the solution very quickly compared to PLGA. In particular, PCP-sp soaked up the water instantly.

3.3 Pore characterization

Figure 4A shows the pore distribution within the scaffolds. PCP-br and PLGA scaffolds had homogeneous pores whereas the pores of PCP-sp covered a wide range of sizes. The porosity and mean pore size of PCP-br were 88.4% and 189 μm, respectively, which were similar to those of PLGA scaffolds prepared by solvent-casting/salt-leaching. On the other hand, freeze-drying-based PCP-sp showed the smallest pore size of ∼ 32 μm.

Figure 4B shows the morphology of porous PLGA-br and PCP-based scaffolds. PCP-br showed no noticeable difference in microstructure compared with that of PLGA-br. PCP-br had 3D porous structures of uniform and distinct square shapes over the surface like PLGA-br. PCP-sp formed a highly porous surface during the freeze-drying process due to the evaporation of ice crystals, but their pores showed smaller and irregular shapes comparing to those of PCP-br and PLGA-br.

3.4 Cell proliferation test

Young chondrocytes from humans were seeded into scaffolds using a static method. Figure 5 shows the SEM images of chondrocytes that were seeded on the inside surface of the scaffold. At day 1 after cell seeding, PCP-br showed the highest cell adhesion rate. Rounded chondrocytes were evenly adhered on the scaffold surfaces. Cells synthesized ECM over a wide area inside the pores over time. In particular, the pores of PCP-br were occupied by synthesized ECM after 7 days. In the case of PCP-sp, initial cell attachment on the scaffolds was high, but cell migration and growth into the center area of the scaffolds were not evidently detected. In contrast, PLGA-br showed

very low cell adhesion at day 1. The pores were barely filled with cell-synthesized ECM even at day 7.

3.5 Chondrogenic tissue formation test

The three types of chondrocyte-seeded scaffolds were allowed to grow for 1, 2, and 4 weeks *in vitro* (Fig. 6). While the tissue volume in PLGA-br apparently did not change for 4 weeks, PCP-br and PCP-sp showed increased tissue volume over time (Fig. 6A). In the case of PCP-sp, tissue was piled up on the surface of the scaffold and the phenomenon appeared distinctly over time. PCP-br showed glossy, yellowish, and a relatively hard cartilage-like tissue based on pinch testing. The compressive strengths of the scaffolds were analyzed over time. Overall, all groups showed lower values compared to those measured before seeding cell because of the decrease in mechanical strength by scaffold swelling and degradation in medium over time. The compressive strength of PCP-br was similar to that of PLGA-br, which was significantly higher than that of PCP-sp (Fig. 6B). However, strength values of cultured scaffolds could not reach to the value of normal cartilage strength.

Histological safranin-O staining (red) exhibited cell distribution within the scaffold and a sustained accumulation of sulfated proteoglycan at the same time (Fig. 6C). The pores of PLGA-br were gradually filled with synthesized ECM, but random cell aggregation was observed over the pores. In PCP-sp, cells grew in the peripheral areas of the scaffolds at week 1. Although cartilage tissue formed inwards within the scaffold, it was predominant at the peripheral areas rather than at the center areas after 2 and 4 weeks. In contrast, PCP-br was stained strongly compared to PCP-sp and PLGA-br. Seeded cells were distributed very well over the pores of the scaffold and produced ECM already at 1 week. Cell-synthesized ECM was increasingly produced over time, and even the areas between pores and the inside of the pores were overspread with ECM in the 4-week cultivation. The magnified images in Fig. 6C show the cell growth tendency at 4 weeks based on scaffold type. Cell growth turned inwards of the scaffolds in PLGA-br and PCP-br with large and regular pores that were clear and interconnected. However, cell filtration was not observed over crushed interconnections in PCP-sp.

3.6 Chondrogenic differentiation

GAG and hydroxyproline contents were analyzed at 1, 2, and 4 weeks. PCP-br showed notably increased GAG content compared to PLGA-br and PCP-sp (Fig. 7A). Moreover, hydroxyproline content in PCP-br was 244 ± 28 μg/mg at 4 weeks, which was significantly higher than that in the other scaffolds (Fig. 7B). The
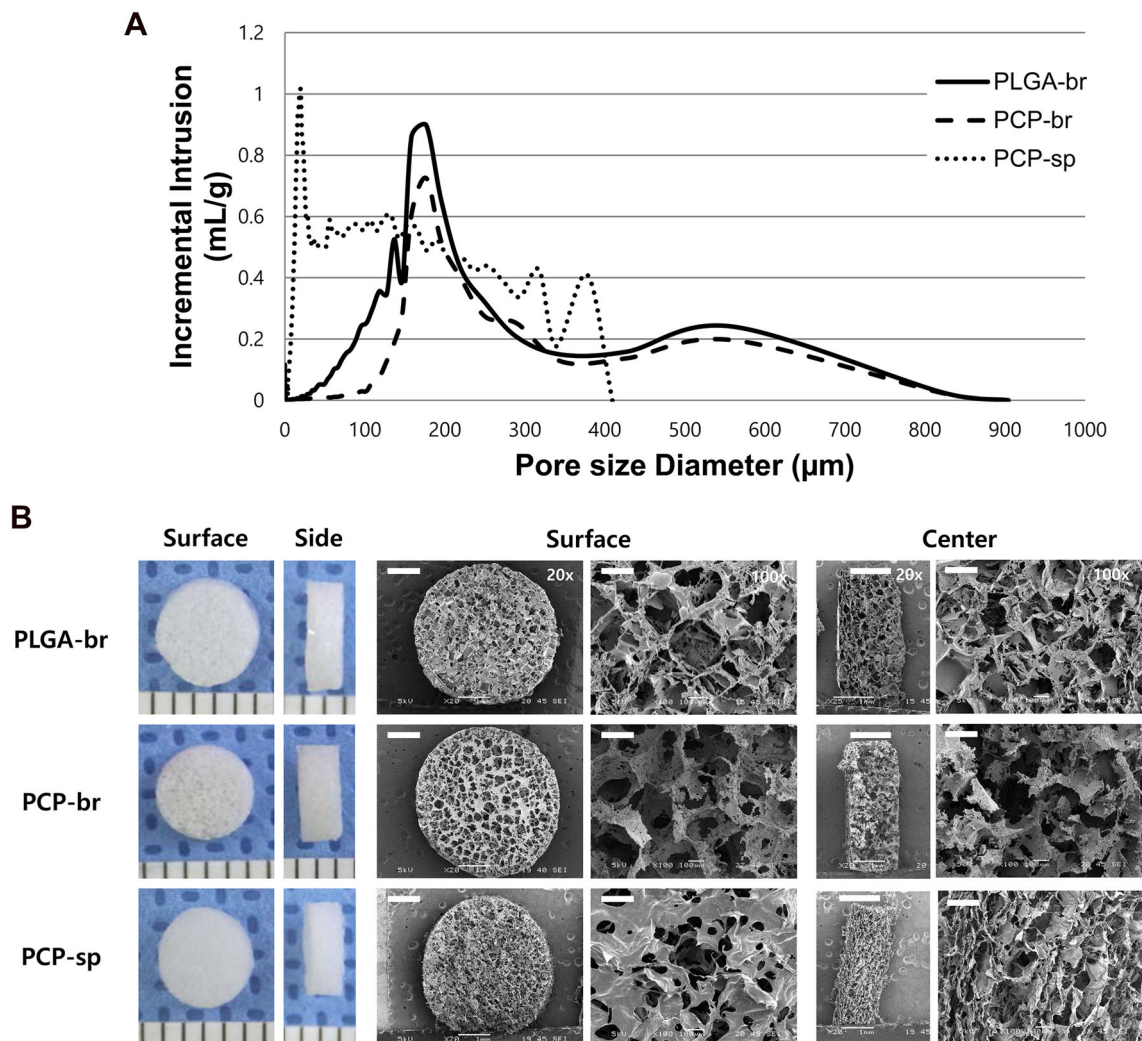
Fig. 4 Pore structure analysis of PLGA-br, PCP-br, and PCP-sp scaffolds. **A** Pore size distribution. **B** Pore morphology (L: gross morphology, R: SEM photomicrographs of the scaffolds; surface, horizontal and vertical cross-section of central areas of scaffolds) of PLGA-br, PCP-br, and PCP-sp scaffolds. Scale unit in gross morphology: mm. Scale bars in SEM images = 1 mm for ×20 and 100 μm for ×100

expression of chondrogenesis-related genes such as type II collagen and aggrecan was analyzed (Fig. 8A). The expression of chondrogenic genes was normalized by GAPDH, a house-keeping gene that is expressed steadily in all specimens (Fig. 8B). The PCP-based scaffolds showed steadily high type II collagen gene levels for 4 weeks. When the mRNA expression was compared between PCP-sp and PCP-br, no significant differences were observed between the two. In turns of aggrecan gene expression, the PCP-based scaffolds showed significantly higher expression than PLGA-br. In particular, the strongest expression of the aggrecan gene was observed in PCP-br.

4 Discussion

As cartilage repair using tissue-derived ECM materials has been investigated actively, we developed mechanically reinforced ECM scaffolds for cartilage tissue engineering. Porous 3D PLGA-br was successfully prepared using the solvent-casting/salt-leaching method. PCP-based scaffolds were also prepared using a common freeze-drying method (for PCP-sp) and modified solvent-casting/salt-leaching method (for PCP-br). Xenogeneic and allogeneic tissues possess the risk of infection and disease transmission. To address this problem, we decellularized PCP before scaffold fabrication and found DNA content of 9.48 ng/mg in PCP after decellularization. Even though it is difficult to remove DNA because of its sticky characteristic and tendency to adhere to ECM proteins [28], our developed
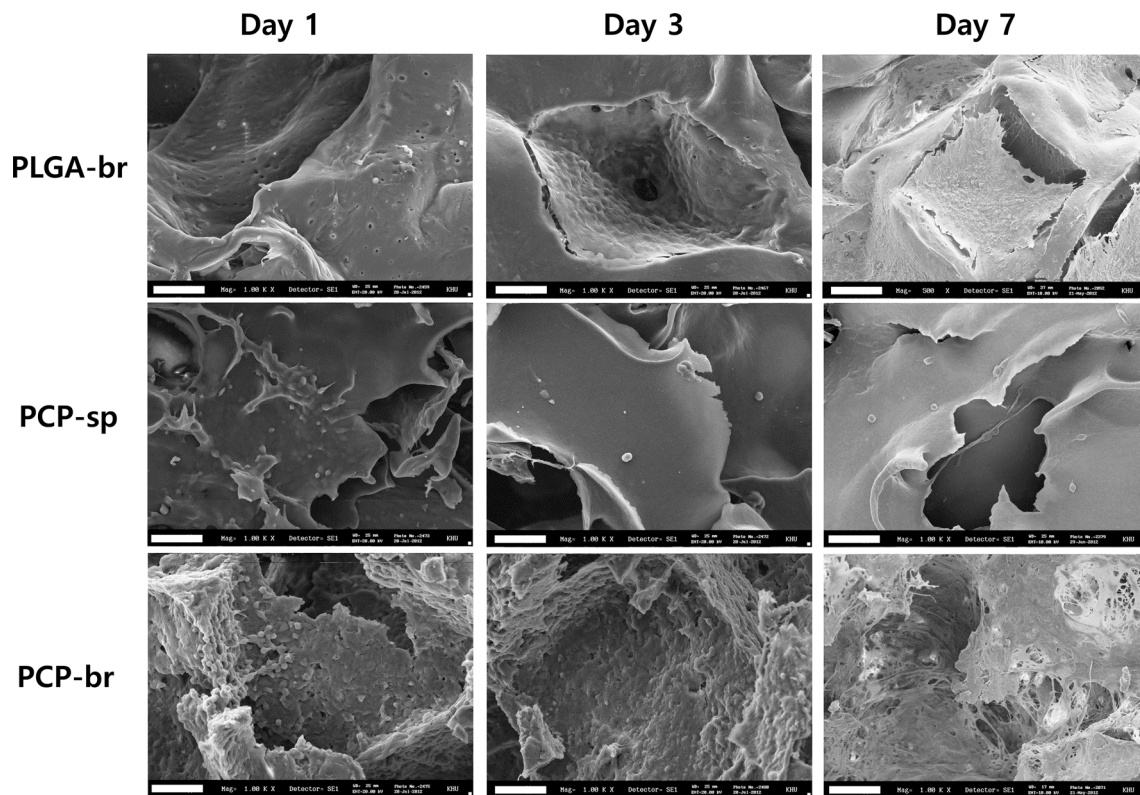
Day 1 **Day 3** **Day 7**

Fig. 5 SEM images of cell adhesion and proliferation. Cell adhesion at day 1 (horizontal cross-section near surface of scaffold) and the tendency of proliferation at day 3 and 7 (horizontal cross-section of central areas of scaffolds). Scale bars = 40 μm

pulverization and chemical and enzymatic combination treatment for decellularization effectively led to very low levels of DNA in the cartilage tissue, removing up to 99.9% of all DNA and resulting in a final DNA level that is comparably lower than those reported in other experiments [29, 30].

Solvent-casting/salt-leaching is a porogen-leaching method used to fabricate a sponge-like porous structure. Synthetic polymers are generally dissolved in an organic solvent and mixed with porogen particles [31, 32]. While salt-leaching could create uniform pores by using salts, the freeze-drying method based on ice crystallization is influenced by the skill and experience of the manufacturer [33, 34]. Scaffolds with non-uniform pore sizes and disordered interconnectivity do not provide the optimal template for cell infiltration and nutrient transfer [35]. Hence, PCP-br was fabricated using a modified solvent-casting/salt-leaching method. In addition, we carried out the crosslinking process twice to enhance the mechanical strength of natural material-based scaffolds.

Generally, carbodiimide stabilized ECM like collagen is employed extensively for the fabrication of biologically active materials. The extracellular matrix (ECM) of tissues is composed of a complex network of proteins, glycoproteins and glycosaminoglycans that surround cells. During carbodiimide mediated crosslinking the carboxylate moiety on one amino acid side chain (Asp, Glu) reacts through a condensation reaction with a primary amine on an adjacent amino acid (Lys). The main advantage of EDC crosslinking is its water solubility, which allows direct bioconjugation without prior organic solvent dissolution. Excess reagent and crosslinking by products are easily removed by washing with water. In particular, the urea by-product formed during the reaction is readily soluble in water and can easily be removed by extraction. Therefore, many previous studies have been done simple washing process after EDC crosslinking for the washing of fabricated scaffolds [36, 37]. Another previous study reported that by systematically modifying the EDC/NHS crosslinking regimes the physical properties of scaffolds can be modulated [38]. This allows discrete control over the mechanical strength and degradation kinetics of the resultant scaffold. In our experiment, even though the first EDC crosslinking at high concentration might require all amines to participate in the reaction, we treated EDC/NHS additionally to form the stable amide bond in scaffolds because limitations of the solid phase and single EDC reaction is inadequate for crosslinking [39, 40]. We confirmed that the PCP-br scaffold cohered chemically via amide bonds from the FTIR results. Mechanical strength test results also
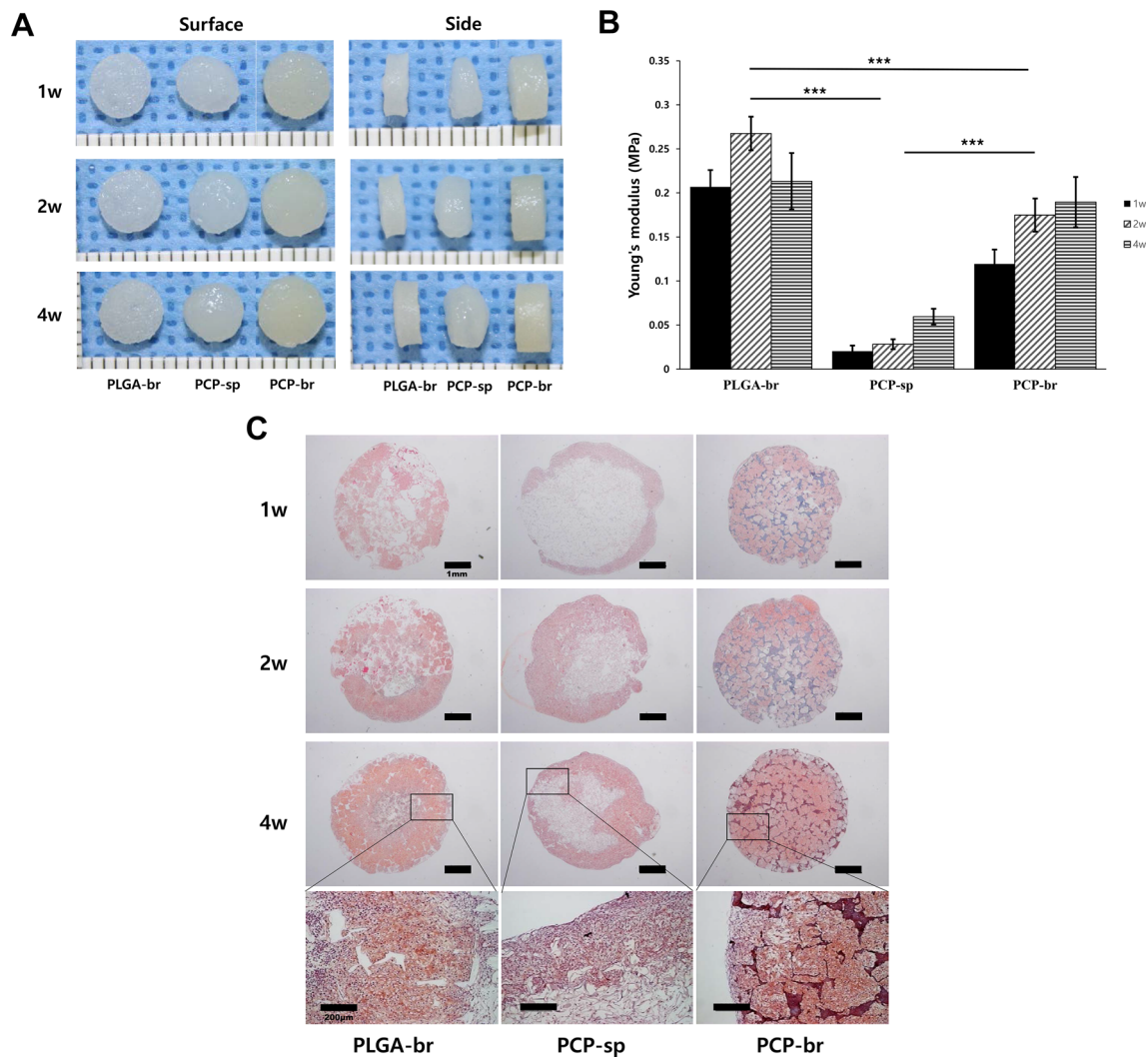
Fig. 6 *In vitro* chondrogenic culture of PLGA-br, PCP-br, and PCP-sp. **A** Gross observation (scale unit, mm). **B** Compressive strengths of cultured PLGA-br, PCP-br, and PCP-sp. **C** Histological analysis of chondrogenic formations at 1, 2, and 4 weeks. Cell growth turned inwards of the scaffolds in PLGA-br and PCP-br with large and regular pores that were clear and interconnected. In particular, PCP-br was stained strongly compared to PCP-sp and PLGA-br
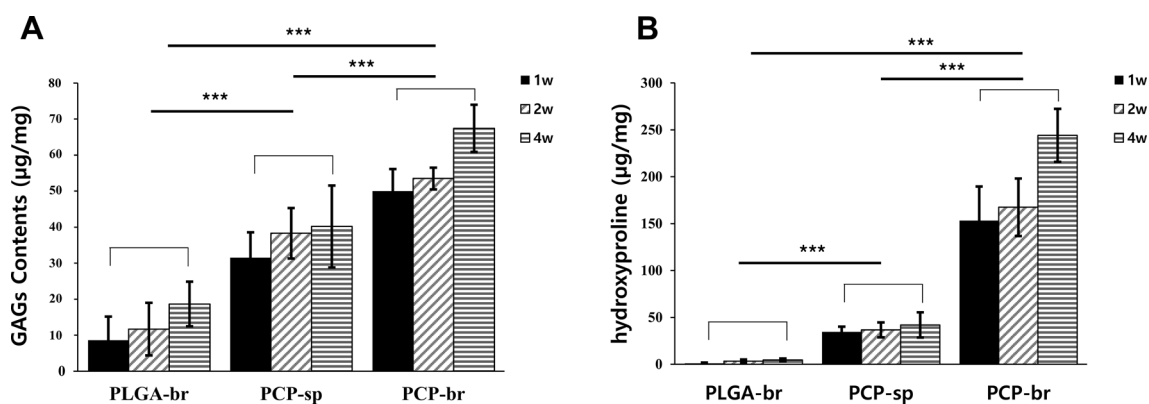

Fig. 7 Chemical analysis for chondrogenesis after 4 weeks of *in vitro* culture. **A** GAG content. **B** Hydroxyproline content. PCP-br showed the highest chondrogenic ECM GAG synthesis among the groups. PCP-br also showed significantly higher hydroxyproline synthesis compared to the other scaffolds. Statistically significant differences: ***$p < 0.001$
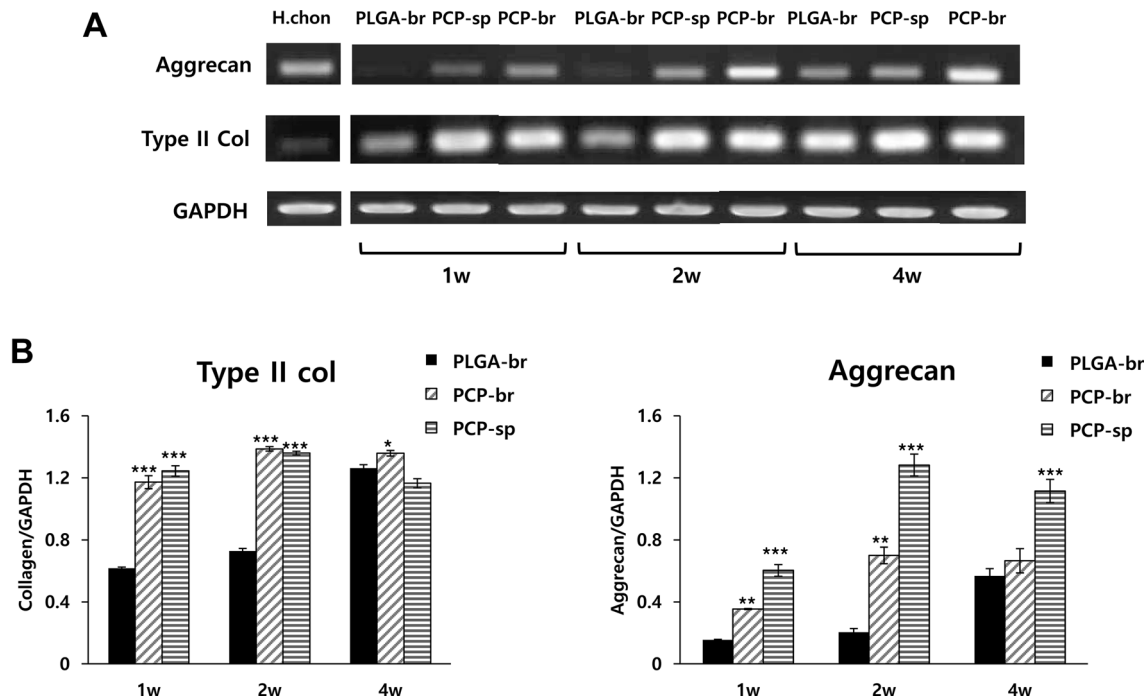
Fig. 8 Analysis of gene expression of aggrecan and type II collagen by RT-PCR. **A** Results of electrophoresis. **B** Quantification of gene expression using Image J program (*$p < 0.05$, **$p < 0.01$, ***$p < 0.001$)

demonstrated that mechanically reinforced PCP-br scaffold showed ∼ 30-fold higher mechanical strength than PCP-sp.

Articular cartilage typically is composed of 68–85% water, 10–20% collagen, and 5–10% proteoglycans. Collagen, as a fibrillar component, is in charge of the structural integrity of the tissue and proteoglycans, as a non-fibrillar component, are in charge of cell–cell interaction, cell adhesion, proliferation, and migration [41]. To find out whether PCP decellularization and PCP-br fabrication processes could change the components of cartilage ECM, we measured hydroxyproline and GAGs contents. Values of hydroxyproline content of PCP-br and native cartilage were 244 ± 28 and 683 ± 25 μg/ml, respectively. However, GAGs content (67 ± 7.4 μg/ml) in PCP-br showed similar amount with that (67 ± 0.3 μg/ml) in native cartilage (data not shown). Therefore, we proved that utilized processes of decellularization and crosslinking did not change the components of cartilage ECM.

Material properties and architecture can affect wettability and absorbency. In comparing the surface wettability of the scaffolds, the PCP-sp (contact angle of 0°) showed the highest wettability, followed by PCP-br (contact angle of 84°) and PLGA-br (contact angle of 134°). The PLGA-br absorbed trypan blue solution very slowly because of the high hydrophobicity of PLGA, whereas the PCP-based scaffolds were easily wetted because of the hydrophilicity of PCP. The negatively charged proteoglycans in the ECM

of native cartilage helped the tissue swell and retain water [29]. The water contact angle of PCP-sp was very low and trypan blue solution permeated more quickly than in PCP-br. This result demonstrates that scaffold fabrication method could affect the wettability of the scaffold. Fabricated PCP-br appeared to have a smooth surface formed by a compressive process, leading to higher surface tension and contact angle compared to those of PCP-sp. Generally, hydrophilic surfaces (contact angle < 90°) become more hydrophilic as the surface roughness increases [42].

In the SEM analysis, PCP-based scaffolds showed higher cell adhesion than did PLGA-br because of PCP's cytophilicity as we had anticipated in the wetting test. However, cell spreading into the scaffolds was different depending on fabrication method, even for the same material. Results from *in vitro* culture showed the contraction of the PCP-sp structure in the medium. The physical weakness of PCP-sp may be the important reason for the limited cell migration and uneven cell distribution, as some studies have proved that chondrocytes prefer rigid matrices for stable adhesions and differentiation [43, 44].

When the expression of genes for cartilage-specific markers were evaluated, bioactive molecules containing PCP-based scaffolds elevated the expression of cartilage-specific markers, type II collagen and aggrecan. Especially, the expression of chondrogenesis-related genes was the highest in PCP-br among the three types of scaffolds. These results demonstrate that material architecture, in

addition to material composition, could influence gene expression and cell function.

Our experiments proved that the behavior of chondrocytes including attachment, cell filtration into scaffolds, and gene expression could be controlled by the components and architecture of the scaffolding material. In addition, the mechanical strength of the developed mechanically reinforced PCP-br (0.89 Mpa) could reach that of native cartilage (0.53–1.34 MPa) [45, 46]. However, our fabrication protocol should be developed. PCP should also be fully characterized like other ECM materials, such as small intestinal submucosa and urinary bladder matrices, to be used in numerous tissue engineering applications in further studies.

In conclusion, we confirmed that combined fabrication methods with crosslinking and modified porogen-leaching for the ECM-based scaffolds improved the mechanical properties and pore structure stability of PCP-br. This fabrication method promoted cell attachment, enhanced inward cell infiltration in the scaffolds, and improved the expression of chondrogenic-specific genes. This study suggests that mechanically reinforced PCP-br could be considered a potential scaffold for *in vitro* tissue-engineered articular cartilage construct.

Compliance with ethical standards

Conflict of interest The authors declare that they have no conflict of interest.

Ethical statement All experimental protocols were approved by the Institutional Review Board at Ajou University (Approval No. AJIRB-MED-SMP-10-266).

References

1. Patra D, Sandell LJ. Antiangiogenic and anticancer molecules in cartilage. Expert Rev Mol Med. 2012;14:e10.
2. Huh SW, Shetty AA, Kim JM, Cho ML, Kim SA, Yang S, et al. Autologous bone marrow mesenchymal cell induced chondrogenesis for the treatment of osteoarthritis of knee. Tissue Eng Regen Med. 2016;13:200–9.
3. Chung C, Burdick JA. Engineering cartilage tissue. Adv Drug Deliv Rev. 2008;60:243–62.
4. Lee J, Im GI. Effects of trichostatin A on the chondrogenesis from human mesenchymal stem cells. Tissue Eng Regen Med. 2017;14:403–10.
5. Mahapatra C, Jin GZ, Kim HW. Alginate-hyaluronic acid-collagen composite hydrogel favorable for the culture of chondrocytes and their phenotype maintenance. Tissue Eng Regen Med. 2016;13:538–46.
6. Chua ILS, Kim HW, Lee JH. Signaling of extracellular matrices for tissue regeneration and therapeutics. Tissue Eng Regen Med. 2016;13:1–12.
7. Jia S, Liu L, Pan W, Meng G, Duan C, Zhang L, et al. Oriented cartilage extracellular matrix-derived scaffold for cartilage tissue engineering. J Biosci Bioeng. 2012;113:647–53.
8. Zhang Y, Yang F, Liu K, Shen H, Zhu Y, Zhang W, et al. The impact of PLGA scaffold orientation on in vitro cartilage regeneration. Biomaterials. 2012;33:2926–35.
9. Choi KH, Song BR, Choi BH, Lee M, Park SR, Min BH. Cartilage tissue engineering using chondrocyte-derived extracellular matrix scaffold suppressed vessel invasion during chondrogenesis of mesenchymal stem cells in vivo. Tissue Eng Regen Med. 2012;9:43–50.
10. Bryant SJ, Anseth KS. Hydrogel properties influence ECM production by chondrocytes photoencapsulated in poly(ethylene glycol) hydrogels. J Biomed Mater Res. 2002;59:63–72.
11. Shin YS, Lee JS, Choi JW, Min BH, Chang JW, Lim JY, et al. Transplantation of autologous chondrocytes seeded on a fibrin/hyaluronic acid composite gel into vocal fold in rabbits: preliminary results. Tissue Eng Regen Med. 2012;9:203–8.
12. Kim HJ, Kim KK, Park IK, Choi BS, Kim JH, Kim MS. Hybrid scaffolds composed of hyaluronic acid and collagen for cartilage regeneration. Tissue Eng Regen Med. 2012;9:57–62.
13. Mahmod SA, Snigh S, Djordjevic I, Yee YM, Yusof R, Ramasamy TS, et al. Phytoestrogen (daidzein) promotes chondrogenic phenotype of human chondrocytes in 2D and 3D culture systems. Tissue Eng Regen Med. 2017;14:103–12.
14. Luo X, Kulig KM, Finkelstein EB, Nicholson MF, Liu XH, Goldman SM, et al. In vitro evaluation of decellularized ECM-derived surgical scaffold biomaterials. J Biomed Mater Res B Appl Biomater. 2017;105:585–93.
15. Guan Y, Liu S, Liu Y, Sun C, Cheng G, Luan Y, et al. Porcine kidneys as a source of ECM scaffold for kidney regeneration. Mater Sci Eng C Mater Biol Appl. 2015;56:451–6.
16. Sreejit P, Verma RS. Natural ECM as biomaterial for scaffold based cardiac regeneration using adult bone marrow derived stem cells. Stem Cell Rev. 2013;9:158–71.
17. Cheng NC, Estes BT, Awad HA, Guilak F. Chondrogenic differentiation of adipose-derived adult stem cells by a porous scaffold derived from native articular cartilage extracellular matrix. Tissue Eng Part A. 2009;15:231–41.
18. Yang Q, Peng J, Guo Q, Huang J, Zhang L, Yao J, et al. A cartilage ECM-derived 3-D porous acellular matrix scaffold for *in vivo* cartilage tissue engineering with PKH26-labeled chondrogenic bone marrow-derived mesenchymal stem cells. Biomaterials. 2008;29:2378–87.
19. Choi BH, Choi KH, Lee HS, Song BR, Park SR, Yang JW, et al. Inhibition of blood vessel formation by a chondrocyte-derived extracellular matrix. Biomaterials. 2014;35:5711–20.
20. Chiang H, Jiang CC. Repair of articular cartilage defects: review and perspectives. J Formos Med Assoc. 2009;108:87–101.
21. Lu L, Zhu X, Valenzuela RG, Currier BL, Yaszemski MJ. Biodegradable polymer scaffolds for cartilage tissue engineering. Clin Orthop Relat Res. 2001;391:S251–70.
22. Bacáková L, Filová E, Rypácek F, Svorcík V, Starý V. Cell adhesion on artificial materials for tissue engineering. Physiol Res. 2004;53:S35–45.
23. Moroni L, de Wijn JR, van Blitterswijk CA. 3D fiber-deposited scaffolds for tissue engineering: influence of pores geometry and architecture on dynamic mechanical properties. Biomaterials. 2006;27:974–85.
24. Nettles DL, Elder SH, Gilbert JA. Potential use of chitosan as a cell scaffold material for cartilage tissue engineering. Tissue Eng. 2002;8:1009–16.

25. Yang Z, Shi Y, Wei X, He J, Yang S, Dickson G, et al. Fabrication and repair of cartilage defects with a novel acellular cartilage matrix scaffold. Tissue Eng Part C Methods. 2010;16:865–76.
26. Liang Q, Wang L, Sun W, Wang Z, Xu J, Ma H. Isolation and characterization of collagen from the cartilage of Amur sturgeon (Acipenser schrenckii). Process Biochem. 2014;49:318–23.
27. Rieppo L, Saarakkala S, Närhi T, Helminen HJ, Jurvelin JS, Rieppo J. Application of second derivative spectroscopy for increasing molecular specificity of Fourier transform infrared spectroscopic imaging of articular cartilage. Osteoarthritis Cartilage. 2012;20:451–9.
28. Gilbert TW, Sellaro TL, Badylak SF. Decellularization of tissues and organs. Biomaterials. 2006;27:3675–83.
29. Elder BD, Eleswarapu SV, Athanasiou KA. Extraction techniques for the decellularization of tissue engineered articular cartilage constructs. Biomaterials. 2009;30:3749–56.
30. Ozeki M, Narita Y, Kagami H, Ohmiya N, Itoh A, Hirooka Y, et al. Evaluation of decellularized esophagus as a scaffold for cultured esophageal epithelial cells. J Biomed Mater Res A. 2006;79:771–8.
31. Liao CJ, Chen CF, Chen JH, Chiang SF, Lin YJ, Chang KY. Fabrication of porous biodegradable polymer scaffolds using a solvent merging/particulate leaching method. J Biomed Mater Res. 2002;59:676–81.
32. Mikos AG, Sarakinos G, Leite SM, Vacanti JP, Langer R. Laminated three-dimensional biodegradable foams for use in tissue engineering. Biomaterials. 1993;14:323–30.
33. Haugh MG, Murphy CM, O'Brien FJ. Novel freeze-drying methods to produce a range of collagen-glycosaminoglycan scaffolds with tailored mean pore sizes. Tissue Eng Part C Methods. 2010;16:887–94.
34. Griffon DJ, Sedighi MR, Schaeffer DV, Eurell JA, Johnson AL. Chitosan scaffolds: interconnective pore size and cartilage engineering. Acta Biomater. 2006;2:313–20.
35. Tan JY, Chua CK, Leong KF. Fabrication of channeled scaffolds with ordered array of micro-pores through microsphere leaching and indirect Rapid Prototyping technique. Biomed Microdevices. 2013;15:83–96.
36. Fiorani A, Gualandi C, Panseri S, Montesi M, Marcacci M, Focarete ML, et al. Comparative performance of collagen nanofibers electrospun from different solvents and stabilized by different crosslinkers. J Mater Sci Mater Med. 2014;25:2313–21.
37. Hu Y, Liu L, Dan W, Dan N, Gu Z, Yu X. Synergistic effect of carbodiimide and dehydrothermal crosslinking on acellular dermal matrix. Int J Biol Macromol. 2013;55:221–30.
38. Grover CN, Cameron RE, Best SM. Investigating the morphological, mechanical and degradation properties of scaffolds comprising collagen, gelatin and elastin for use in soft tissue engineering. J Mech Behav Biomed Mater. 2012;10:62–74.
39. Young JJ, Cheng KM, Tsou TL, Liu HW, Wang HJ. Preparation of cross-linked hyaluronic acid film using 2-chloro-1-methylpyridinium iodide or water-soluble 1-ethyl-(3,3-dimethylaminopropyl)carbodiimide. J Biomater Sci Polym Ed. 2004;15:767–80.
40. Staros JV, Wright RW, Swingle DM. Enhancement by N-hydroxysulfosuccinimide of water-soluble carbodiimide-mediated coupling reactions. Anal Biochem. 1986;156:220–2.
41. Cohen NP, Foster RJ, Mow VC. Composition and dynamics of articular cartilage: structure, function, and maintaining healthy state. J Orthop Sports Phys Ther. 1998;28:203–15.
42. Wenzel RN. Resistance of solid surfaces to wetting by water. Ind Eng Chem. 1936;28:988–94.
43. Discher DE, Janmey P, Wang YL. Tissue cells feel and respond to the stiffness of their substrate. Science. 2005;310:1139–43.
44. Kong HJ, Polte TR, Alsberg E, Mooney DJ. FRET measurements of cell-traction forces and nano-scale clustering of adhesion ligands varied by substrate stiffness. Proc Natl Acad Sci U S A. 2005;102:4300–5.
45. Athanasiou KA, Agarwal A, Dzida FJ. Comparative study of the intrinsic mechanical properties of the human acetabular and femoral head cartilage. J Orthop Res. 1994;12:340–9.
46. Athanasiou KA, Rosenwasser MP, Buckwalter JA, Malinin TI, Mow VC. Interspecies comparisons of in situ intrinsic mechanical properties of distal femoral cartilage. J Orthop Res. 1991;9:330–40.